



## Full Length Article

## Time-resolved synchrotron light source X-ray detection with Low-Gain Avalanche Diodes

G.T. Saito <sup>a,\*</sup>, M. Leite <sup>a</sup>, S.M. Mazza <sup>b</sup>, Y. Zhao <sup>b</sup>, T. Kirkes <sup>b</sup>, N. Yoho <sup>b</sup>, D. Yerdea <sup>b</sup>, N. Nagel <sup>b</sup>, J. Ott <sup>b</sup>, M. Nizam <sup>b</sup>, M. Morales <sup>c</sup>, H.F.-W. Sadrozinski <sup>b</sup>, A. Seiden <sup>b</sup>, B. Schumm <sup>b</sup>, F. McKinney-Martinez <sup>b</sup>, G. Giacomini <sup>d</sup>, W. Chen <sup>d</sup>

<sup>a</sup> Universidade de São Paulo, São Paulo, SP, Brazil

<sup>b</sup> SLIPP, University of California Santa Cruz, 1156 High Street, Santa Cruz, CA, United States

<sup>c</sup> IPEN-CNEN, São Paulo, SP, Brazil

<sup>d</sup> Brookhaven National Laboratory, Upton, NY, United States

## ARTICLE INFO

## Keywords:

Ultra-fast silicon sensors  
Low-Gain Avalanche Diodes  
Charge multiplication  
Thin tracking sensors  
Synchrotron instrumentation

## ABSTRACT

Low Gain Avalanche Diodes (LGADs) represent the state-of-the-art in timing measurements and will instrument future timing detectors at the High Luminosity Large Hadron Collider (HL-LHC) experiments. While conceived as a sensor for charged particles, the intrinsic gain of LGADs makes it possible to detect low energy X-rays with good energy resolution and excellent timing (tens of picoseconds). Using the Stanford Synchrotron Radiation Lightsource (SSRL) at SLAC, several LGADs designs were characterized with energies from 5 to 35 keV. The SSRL provides 10 ps pulsed X-ray bunches separated by 2.1 ns intervals, and with an energy dispersion ( $\Delta E/E$ ) of  $1 \times 10^{-4}$ . LGADs fabricated by Hamamatsu Photonics (HPK) and Brookhaven National Laboratory (BNL) with different thicknesses ranging from 20  $\mu\text{m}$  to 50  $\mu\text{m}$  and different gain layer designs were read out a two stage fast amplification circuit and digitized with a high bandwidth, high sampling rate oscilloscope. PIN devices from HPK were characterized as well. A systematic and detailed characterization of the devices' energy linearity, resolution and timing resolution as a function of X-ray energy was performed for different biasing voltages at room temperature.

## 1. Introduction

Low-Gain Avalanche Diodes (LGAD) were originally developed to be used as sensors in the timing detectors of both ATLAS and CMS experiments at the LHC [1,2]. These silicon detectors offer a time resolution of tens of picoseconds for measuring charged particles by means of a gain layer that provides an intrinsic moderate gain [3]. If maintained these characteristics when measuring X-ray photons, these devices could be used as Synchrotron X-ray detectors capable of resolving short pulses in a high repetition rate beam in a broad range of energies. In this work we report the response of different designs of LGADs in a 500 MHz repetition rate of 10 ps X-ray pulses Synchrotron beamline in energies between 5 keV and 35 keV.

## 2. Devices tested

LGADs are thin silicon sensors composed by the bulk, a low-doped volume, typically between 20  $\mu\text{m}$  and 50  $\mu\text{m}$  and a highly doped thin layer (gain layer) just below the PN junction of the device. On Table 1,

the nominal bulk thickness and the depth of the gain layer of the 3 LGADs used on this test (HPK 3.1, HPK 3.2 and BNL 20um) and a PIN diode (HPK PIN) is presented. All 4 sensors are single pad devices having an nominal active area of  $1.3 \times 1.3 \text{ mm}^2$ .

## 3. Setup at SLAC SSRL

For this test, Beamline 11-2 of the Stanford Synchrotron Radiation Lightsource (SSRL) at SLAC [4] was used for this test. It provides a X-ray beam with energy dispersion  $\Delta E/E$  of  $1 \times 10^{-4}$ . The bunches are about 10 ps wide and separated by 2.1 ns. They are bundled in 4 groups of 70 bunches, as seen on Fig. 1. Before the 4 groups there is an isolated bunch that is kept in phase with the signal used as a trigger in this setup.

The 4 devices tested were mounted on PCBs with a  $\approx 2 \text{ GHz}$  bandwidth TIA amplifier, described on [5], and digitized by a 13 GHz bandwidth 128 GS/s sampling rate oscilloscope.

\* Corresponding author.

E-mail address: [g.saito@cern.ch](mailto:g.saito@cern.ch) (G.T. Saito).

<https://doi.org/10.1016/j.nima.2024.169454>

Received 16 November 2023; Received in revised form 5 April 2024; Accepted 13 May 2024

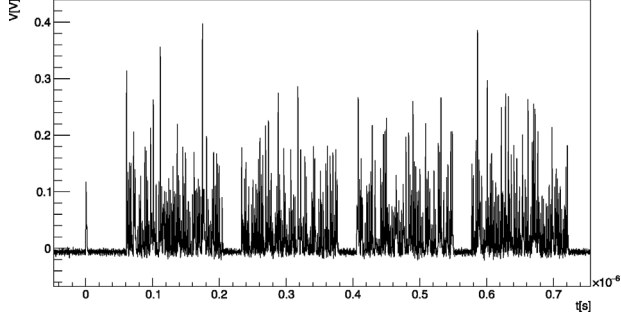
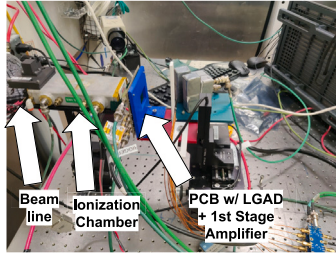
Available online 16 May 2024

0168-9002/© 2024 Elsevier B.V. All rights are reserved, including those for text and data mining, AI training, and similar technologies.

**Table 1**

Main characteristics of tested HPK and BNL LGADs and PIN.

Device	Breakdown	Active thickness	Gain layer
HPK 3.1	230 V	50 $\mu\text{m}$	shallow
HPK 3.2	130 V	50 $\mu\text{m}$	deep
HPK PIN	400 V	50 $\mu\text{m}$	no gain
BNL 20um	100 V	20 $\mu\text{m}$	shallow

**Fig. 1.** Waveform acquired on the oscilloscope with a HPK 3.1 LGAD showing the bunch structure of the SSRL. The four groups of 70 bunches following the single isolated bunch can be identified on the figure.**Fig. 2.** The setup in front of SSRL 11-2 beamline showing the ionization chamber and the PCB holding the devices under test.

As show by Fig. 2, the PCB was positioned just in front of a ionization chamber, used to measure the beam intensity. All of the devices were kept inside an electromagnetic shielding soldered to the PCB providing a light tight enclosure and operated at room temperature.

## 4. Analysis

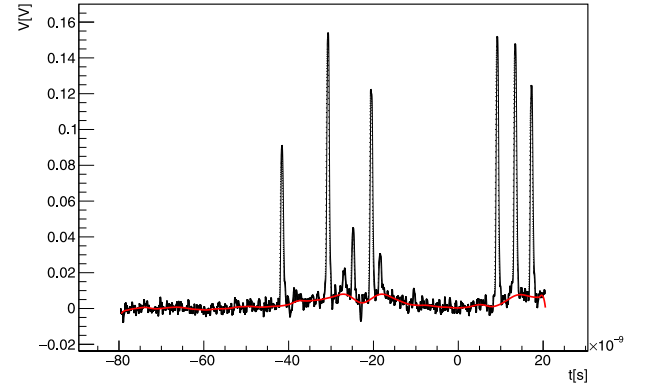
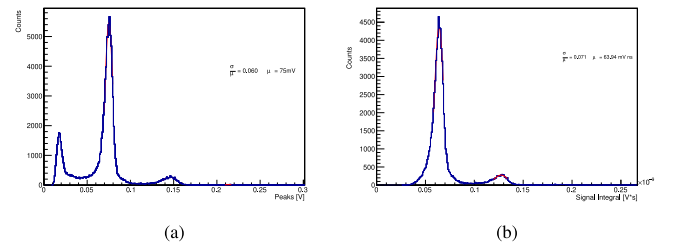
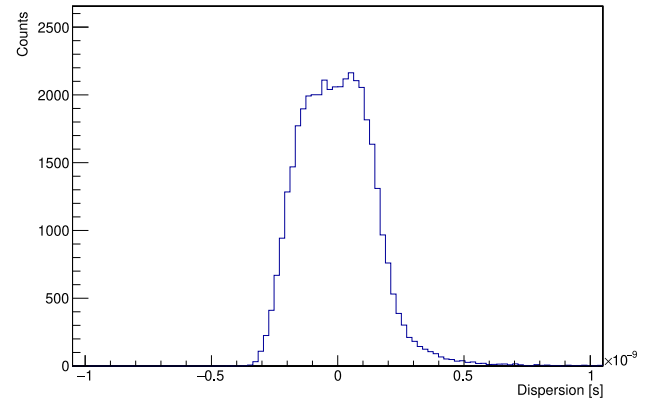
### 4.1. Peak finding

To probe the energy response and time resolution of these devices, an analysis of the transient signal characteristics was performed. An example of waveform acquired by the oscilloscope is shown by Fig. 3. While the individual peaks can be distinguished, a significant baseline shift is present in the waveform, affecting the response of the devices. To correct for this effect, a signal processing method from spectroscopy, called *asymmetrically re-weighted penalized least squares smoothing* [6] was performed for all acquired waveforms, in order to evaluate and subtract the baseline shift (red curve in Fig. 3).

To identify the individual transient signals from the devices, the noise in the empty leading interval is calculated and used as threshold (7 times the noise) to select signals. a cut of  $7\sigma$  is performed. Furthermore, two neighboring peaks should be separated by at least 2.1 ns to be considered valid peaks.

### 4.2. Energy estimation

Both the pulse amplitude and area were utilized as estimators of the energy of the absorbed X-ray when assessing the energy linearity and resolution of the devices.

**Fig. 3.** Oscilloscope acquired waveform from a HPK 3.1 LGAD sensor biased at 200 V when exposed to a beam of 35 keV X-rays and acquired by the oscilloscope. The baseline estimation (red curve) follows the procedure described in the text.**Fig. 4.** Distribution of signal amplitude (a) and signal area (b) of a HPK type 3.1 LGAD sensor biased at 100 V exposed to a beam of 35 keV X-rays. The red curves are Gaussian fits on the tallest peak.**Fig. 5.** Distribution of CFD corrected signal phases in relation to the 2.1 ns bunch separation of SSRL. This example is for a HPK type 3.1 LGAD at 200 V exposed to a beam of 35 keV X-rays.

#### 4.2.1. Pulse amplitude

After identifying the individual peaks, all of the amplitudes of these peaks for a given operating condition are represented in a histogram and a Gaussian fit is performed in the tallest peak of the distribution. An example of such distribution for a HPK type 3.1 LGAD biased at 100 V, exposed to a beam of 35 keV is shown on Fig. 4(a). From the Gaussian fit, it is extracted the average  $\mu$  and standard deviation  $\sigma$ , to be used as the energy estimator ( $\mu$ ) and as the energy resolution ( $\frac{\sigma}{\mu}$ ) of the device.

#### 4.2.2. Pulse area

Another manner in which information from the signal can be used to estimate the energy of the absorbed X-ray is by calculating the area of the pulse shape. This area is numerically calculated using a window

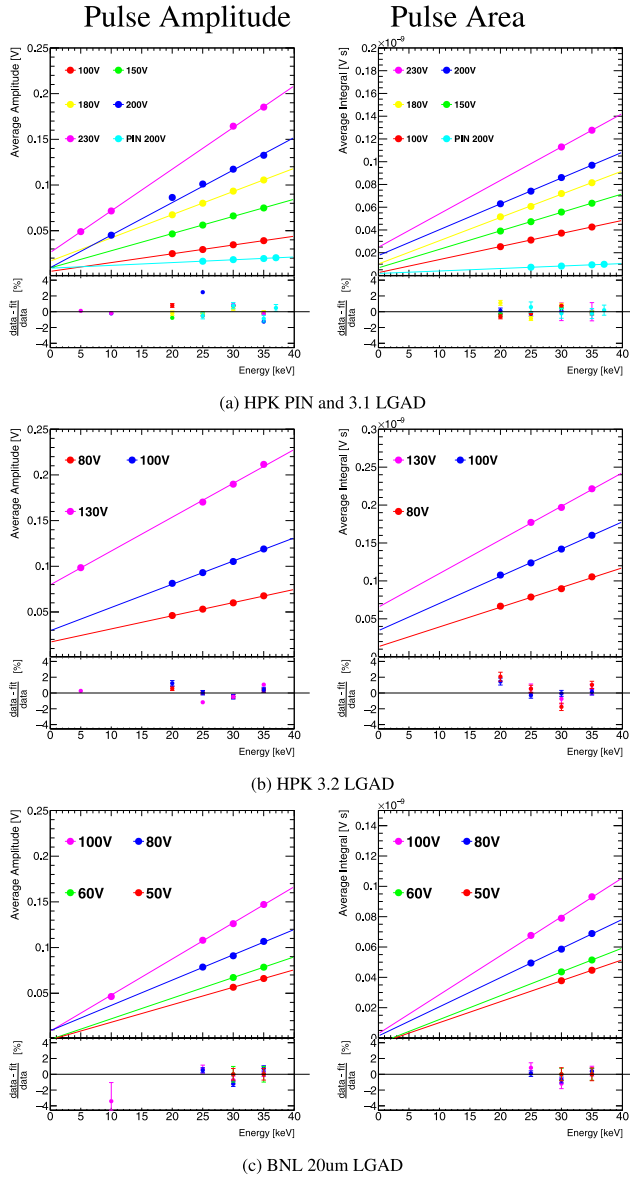


**Fig. 6.** The energy response for the 3 LGADs and PIN tested is shown on the upper part of the plots. Each point is the average signal amplitude (left) or area (right) of a device when exposed to a monochromatic beam at constant bias voltage. The lines are linear fits for a same bias voltage showing the linearity of the sensor response as function of X-ray energy. The lower plots show the dispersion of the points around the linear fit.

of 2 ns centered on the pulse maximum value. The same procedure for filling a histogram when using the pulse amplitude is performed and the Gaussian fit parameters used as energy estimation and resolution. One of these distributions can be seen on Fig. 4(b).

#### 4.3. Time resolution

To estimate the time resolution of LGADs when detecting X-rays in a Synchrotron, the synchronous nature of the bunch structure inside the accelerator can be used to provide very precise information about the timing of the X-ray detection on the devices. As detailed on Section 3 the SSRL provides bunches of 10 ps duration separated by 2.1 ns [4].

The time of each individual signal is calculated using a Constant Fraction Discriminator (CFD) at 20% and the time marking of each signal modulo 2.1 ns is used to fill an histogram as shown on Fig. 5.

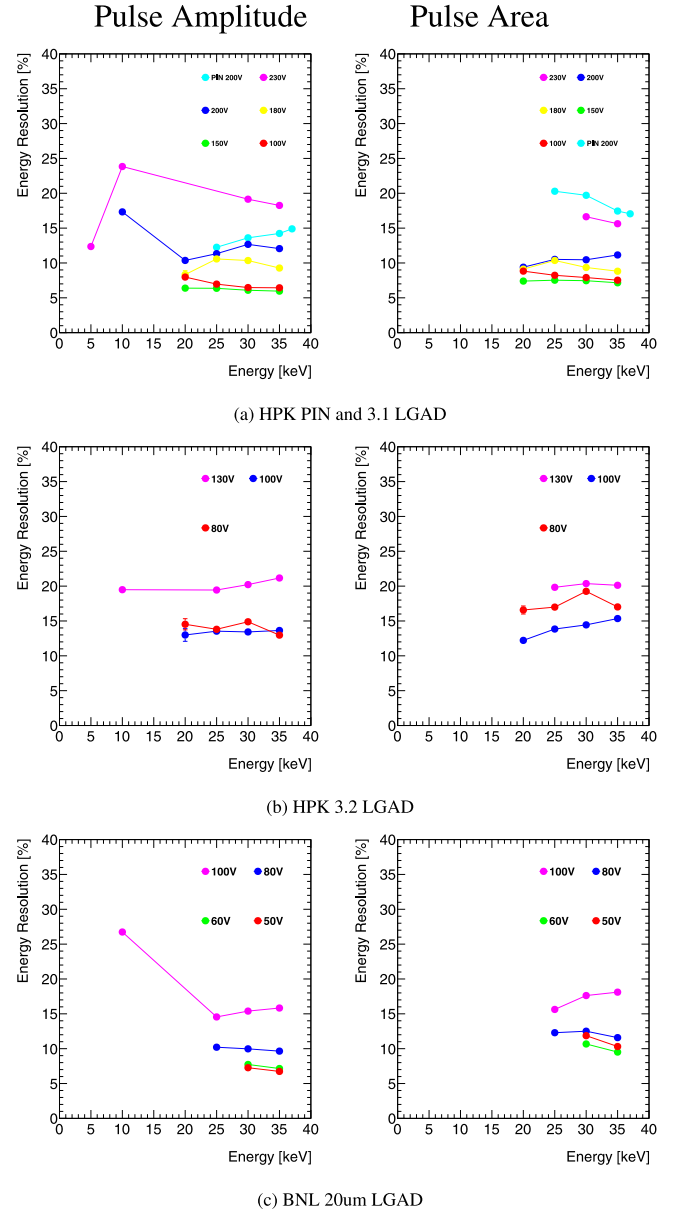


**Fig. 7.** The energy resolution of each of the 3 LGADs and PIN tested. Each point is the ratio  $\frac{\sigma}{\mu}$  for the Gaussian fit on the distributions of signal amplitude (left) and area (right).

The standard deviation of this distribution is used as an estimation of the device time resolution for X-rays.

## 5. Results

### 5.1. Energy linearity

The energy linearity of the devices is shown on Fig. 6. Each point represents the signal average amplitude (plots on the left) or area (right) for the devices exposed to a monochromatic beam at constant bias voltage. For the set of measurements in a same bias voltage a linear fit is performed to evaluate the linearity of the device response at each chosen bias. The points on the lower plots are the dispersion around the linear fit. The energy response linearity, for both the analysis using the signal amplitude and for using the area, it is within 6%.

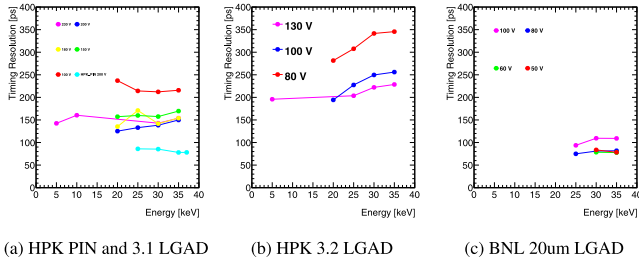


**Fig. 8.** Time resolution of all 4 devices tested as function of the X-ray beam energy for different bias voltages. The time resolution is calculated using a CFD at 20% fraction and the bunch structure inside the SSRL.

### 5.2. Energy resolution

The energy resolution of the tested devices is presented on Fig. 7, the points are the ratio  $\frac{\sigma}{\mu}$  from the Gaussian fit parameters, explained on Section 4.2, using the signal amplitude (plots on the left) and the area (right).

It can be seen that for lower bias voltages and for the PIN diode that have overall lower signal to noise ratio, the area method has a worse energy resolution when compared to the pulse amplitude method. For higher bias voltages there is almost no difference between the pulse amplitude and area analysis methods. Also, when comparing the same X-ray energy, all 3 LGADs can achieve a better energy resolution than the PIN diode for a lower to moderate bias voltage, as at higher voltages, fluctuations on the gain start to widen the amplitude and integral distributions.

### 5.3. Time resolution

Fig. 8 presents the time resolution for the devices tested, using the analysis technique explained on Section 4.3 and information on the bunch structure inside the SSRL.

The PIN diode (light blue) has a better time resolution than both 50  $\mu\text{m}$  thick HPK LGADs. This can be explained as the PIN signal has no dependence on the depth of photon absorption [7]. The thinner 20  $\mu\text{m}$  BNL LGAD presents a 60 to 100 ps time resolution, or as good as the PIN diode tested.

## 6. Conclusions

To use time-resolved techniques for X-ray detection in Synchrotrons light applications, the sensors should be able to discriminate signals in time up to the repetition rate of the machine and be capable of extracting energy information from the incoming X-rays. The tested

devices were able to resolve in time the 500 MHz rate of the SSRL beam line with a time resolution between 60 ps and 350 ps.

Regarding energy estimation, LGADs can estimate the photon energy with a resolution between 6% and 20%, and a linearity better than 6%, indicating the possibility of these devices replacing silicon PIN diodes detectors with a better energy resolution at low energies.

The thin 20  $\mu\text{m}$  active volume BNL LGAD was the only design capable of performing sub-100 ps time resolution, much better than the 50  $\mu\text{m}$  HPK LGADs achieved, and as good as the 60 ps to 70 ps time resolution of the PIN.

Regarding the usage of the signal amplitude or the area as energy estimator, it is shown that for conditions with a small signal to noise ratio, there is a worsening of the energy resolution when using the area method, but no change is seen for data with higher signal to noise ratio.

### Declaration of competing interest

The authors declare that they have no known competing financial interests or personal relationships that could have appeared to influence the work reported in this paper.

### Acknowledgments

This work was supported by the United States DoE, grant DE-FG02-04ER41286, CACTUS DJ-LGAD SBIR. Use of the Stanford Synchrotron Radiation Lightsource, SLAC National Accelerator Laboratory, is supported by the U.S. DoE Office of Science, Office of Basic Energy Sciences under Contract No. DE-AC02-76SF00515. The authors acknowledge support from FAPESP, Brazil (grant 2020/04867-2), CNPq, Brazil (INCT 406672/2022-9), and CAPES, Brazil.

### References

- [1] ATLAS Collaboration, Technical Design Report: A High-Granularity Timing Detector for the ATLAS Phase-II Upgrade, Technical Report, CERN, Geneva, 2020, URL <https://cds.cern.ch/record/2719855>.
- [2] C. CMS, A MIP Timing Detector for the CMS Phase-2 Upgrade, Technical Report, CERN, Geneva, 2019, URL <https://cds.cern.ch/record/2667167>.
- [3] H.-W. Sadrozinski, et al., Ultra-fast silicon detectors (UFS), Nucl. Instrum. Methods Phys. Res. A 831 (2016) 18–23, <http://dx.doi.org/10.1016/j.nima.2016.03.093>.
- [4] SLAC, Stanford synchrotron radiation lightsource, 1973, URL <https://www-ssrl.slac.stanford.edu>.
- [5] A. Seiden, et al., Potential for improved time resolution using very thin ultra-fast silicon detectors (UFSs), 2021, [arXiv:2006.04241](https://arxiv.org/abs/2006.04241).
- [6] S.-J. Baek, A. Park, Y.-J. Ahn, J. Choo, Baseline correction using asymmetrically reweighted penalized least squares smoothing, Analyst 140 (2015) 250–257, <http://dx.doi.org/10.1039/C4AN01061B>.
- [7] S. Mazza, et al., Synchrotron light source X-ray detection with low-gain avalanche diodes, J. Instrum. 18 (10) (2023) P10006, <http://dx.doi.org/10.1088/1748-0221/18/10/P10006>.